PAN
ARCHIVES OF ACOUSTICS
Vol. **45**, No. 3, pp. 385–391 (2020)
DOI: 10.24425/aoa.2020.134055

Research Paper

Effect of Pipe Bends on the Low-Frequency Torsional Guided Wave Propagation

Wenjun WU[(1),(2)*], Junhua WANG[(1)]

[(1)] *Wuchang University of Technology*
Wuhan 430223
*Corresponding Author e-mail: wuweju@126.com; wuwenjun@whut.edu.cn

[(2)] *School of Energy and Power Engineering*
Wuhan University of Technology
Wuhan 430063

(*received December 31, 2019; accepted May 27, 2020*)

Wave motion in pipe bends is much more complicated than that in straight pipes, thereby changing considerably the propagation characteristics of guided waves in pipes with bends. Therefore, a better understanding of how guided waves propagate in pipe bends is essential for inspecting pipelines with bends. The interaction between a pipe bend and the most used non-dispersive torsional mode at low frequency in a small-bore pipe is studied in this paper. Experiments are conducted on a magnetostrictive system, and it is observed that T(0,1) bend reflections and mode conversions from T(0,1) to F(1,1) and F(2,1) occur in the pipe bend. The magnitude of the T(0,1) bend reflections increases with increasing propagation distance and excitation frequency. The amplitude of the mode-converted signals also increases with increasing propagation distance, but it decreases with increasing excitation frequency. Because of their longer bent path, the test signals for a pipe bend with a bending angle of 180° are much more complicated than those for one with a bending angle of 90°. Therefore, it is even more difficult to scan a bent pipe with a large bending angle. The present findings provide some insights into how guided waves behave in pipe bends, and they generalize the application of guided-wave inspection in pipelines.

Keywords: guided wave; torsional mode; pipe bends; mode conversion.

1. Introduction

Ultrasonic guided wave technique (Rose, 1999; He *et al.*, 2001; Ta *et al.*, 2004) has been widely used in the nondestructive testing of long straight pipes for its wide detection coverage and high scanning efficiency. However, in most practical applications the tested pipeline contains bends, thereby complicating the guided wave based inspection significantly. Pipe bends affect the propagation of guided waves. When an incident mode travels through a pipe bend, complex interactions occur between the two, thereby scattering guided waves in other mode. Thus, different modes will overlap with each other, confusing the interpretation of test signals and even making the inspection impractical.

In typical guided wave inspections, only one dominant mode is selected for excitation in the pipe to avoid different modes overlapping. Torsional modes [e.g., T(0,1)] and longitudinal modes [e.g., L(0,1) and L(0,2)] are the most used probing modes because of their non-dispersive or low-dispersive and simple excitation. The interactions between pipe bends and these probing modes have been discussed in some studies (Demma, *et al.*, 2001; Sanderson *et al.*, 2013; Zhou, Ichchou, 2010; Nishino *et al.*, 2006; Verma *et al.*, 2014). Demma *et al.* (2001) simulated the propagations of the L(0,2) and T(0,1) modes passing through a pipe bend by using the finite element method, and they studied the transmission coefficients of the L(0,2) mode with respect to the bending radius. Also by using the finite element method, Sanderson *et al.* (2013) investigated the mode conversions of the T(0,1) mode guided wave at bends and further analyzed the energy focusing of the T(0,1) mode in the bend. Zhou and Ichchou (2010) numerically simulated the propagation of a guided wave in pipes containing bends using the wave finite element method and studied the trans-

mission coefficients of guided waves passing through bends. Nishino *et al.* (2006) experimentally investigated the interaction of L(0,1) mode with a pipe bend using a wideband laser ultrasonic system. They found that part of the L(0,1) mode is converted to the F(1,1) mode when passing through the bends, and the amplitude of F(1,1) mode, converted from the L(0,1) mode, increases with increasing bending angle. Verma *et al.* (2014) excited the L(0,2) mode in a pipe with a magnetostrictive transducer and studied the effects of bending angle and bending radius on the mode conversion and transmission coefficients of the L(0,2) mode.

Despite some preliminary studies, the effect of bends on the guided wave propagation remains poorly understood. In the present study, a small-bore pipe is investigated because (i) very little work has been done on such pipes and (ii) waves in small-bore pipes behave relatively simply, especially at the low frequency where only three modes exist, namely the longitudinal L(0,1) mode, the torsional T(0,1) mode and the flexural F(1,1) mode. The L(0,1) and T(0,1) modes are usually used as probing modes, and the T(0,1) has attracted increasing attention in recent years because of its non-dispersive nature. In the present work, the interaction of the low-frequency mode T(0,1) with a pipe bend is studied experimentally on a magnetostrictive system. Section 2 presents the dispersion curves of guided waves in pipe bends calculated by using semi-analytical finite element (SAFE) method. Section 3 reports on experiments performed according to the dispersion curves, presenting the experimental results and analyzing them.

2. Dispersion curves for guided waves in pipe bends

2.1. SAFE method (Hayashi *et al.*, 2005)

According to the principle of virtual work, the governing equation for a guided wave is

$$\int_V \delta\boldsymbol{\varepsilon}^{\mathrm{T}}\boldsymbol{\sigma}\,\mathrm{d}V + \int_V \delta\mathbf{u}^{\mathrm{T}}\rho\ddot{\mathbf{u}}\,\mathrm{d}V = 0, \tag{1}$$

where $\boldsymbol{\varepsilon}$, $\boldsymbol{\sigma}$, and $\mathbf{u}$ stand for the stress, strain, and displacement, respectively, and $\ddot{\mathbf{u}}$ is the second derivative of displacement with respect to time. The integration in Eq. (1) is three-dimensional, so the calculation of Eq. (1) is large when calculating with the finite element method. Considering the harmonic propagation in the longitudinal direction, the displacement vector at any point in a pipe bend satisfies

$$\mathbf{u} = \mathbf{U}(r,\theta)\exp(ikz')\exp(-i\omega t), \tag{2}$$

where (r,θ,z') are the toroidal coordinates, (r,θ) are the polar coordinates of the cross section of the pipe bend, and the z' axis coincides with the pipe centerline. Also, k is for the wavenumber and ω is the angular frequency. Substituting Eq. (2) into Eq. (1), the three-dimensional integration in Eq. (1) is reduced to the two-dimensional integration of the cross section of the pipe bend, thereby reducing the calculation significantly. Refer to (Hayashi *et al.*, 2005) for detailed derivations.

2.2. Dispersion curves for guided wave in bended pipe

This study employs a stainless steel (oCr18Ni9) pipe (density: 7930 kg/m^3; Young's modulus: 206 GPa; Poisson ratio: 0.27) with an outer diameter of 22 mm, a wall thickness of 2 mm, and a bending radius of 75 mm. The dispersion curves for guided waves in this pipe bend are calculated by using the SAFE method (Hayashi *et al.*, 2005). The cross section of the pipe bends is meshed with 48 elements in circumference and two elements in thickness. The element dimensions are much smaller than the wavelength of the guided waves used in this case, and thus the computational results are convergent and accurate.

The group-velocity dispersion curves for (a) a straight pipe and (b) a pipe bend are shown in Fig. 1. Compared with the dispersion curve for a straight pipes, that for a pipe bend differs significantly. Firstly, the $\mathrm{L}_C(0,1)$ and $\mathrm{T}_C(0,1)$ modes in a pipe bend have a cut-off frequency that does not occur for the corresponding modes [L(0,1) and T(0,1)] in a straight pipe. Second,

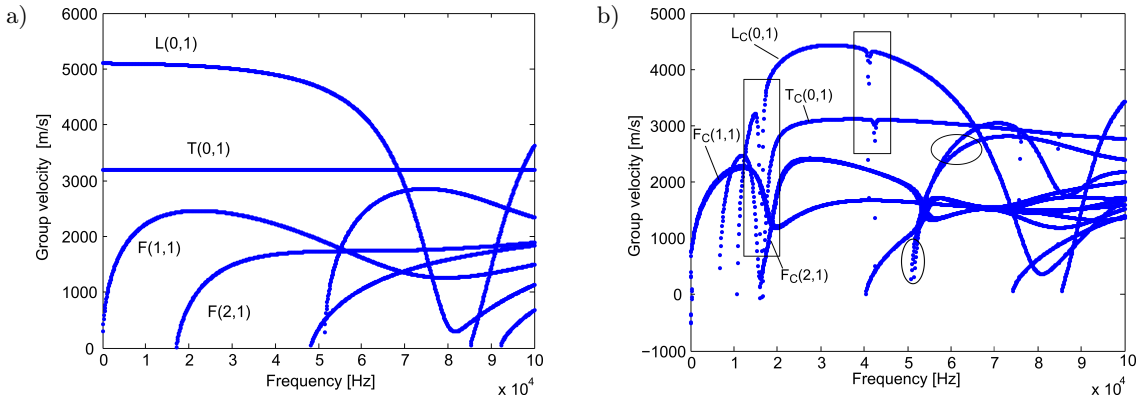

Fig. 1. Group-velocity dispersion curves for: a) straight pipe and b) pipe bend.

the dispersion curve for a pipe bend exhibits "mode splitting" as indicated by the circle in Fig. 1b and interpreted well by Demma *et al.* (2005). Because the pipe bend is not axisymmetric, the originally identical mode indicated by a single dispersion curve in a straight pipe is no longer identical but splits into two modes that differ depending on the orientation of their mode shape. Finally, the dispersion curve for a pipe bend exhibits "mode repulsion" as marked by the rectangle in Fig. 1b and observed similarly in the dispersion curves for plates (Überall *et al.*, 1994), curved plates (Bao *et al.*, 1999; Maze *et al.*, 1999), helical waveguides (Treyssede, 2008), and rails (Loveday *et al.*, 2018), among others. These aforementioned phenomena will definitely affect the propagation of waves in pipe bends, and should be accounted for in guided wave inspections.

3. Experiments and analysis

Experiments were conducted by using a magnetostrictive system to investigate the effect of pipe bends on the propagation of the torsional T(0,1) mode.

3.1. Experimental setup

A schematic diagram of the experimental configuration is shown in Fig. 2. The signals generated by a function generator and then amplified by a power amplifier were sent to the transmitting transducer and excited the waves in the pipe. Incident waves propagated along the pipe and were sensed by the receiving transducer. The received signals were then pre-amplified, transformed from analog to digital, and sent to a laptop for analysis.

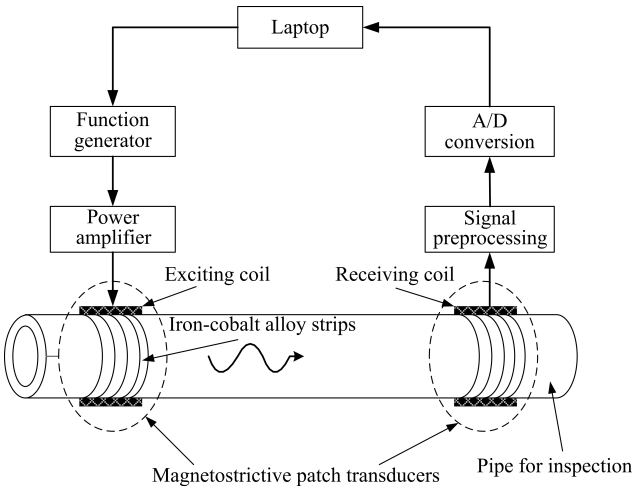

Fig. 2. Schematic of experimental configuration (Wu, Wang, 2019).

In this experiment, a magnetostrictive patch transducer was used to excite torsional waves. According to the Wiedemann effect, two magnetic fields of comparable magnetic intensity should be applied in the circumferential and axial directions, respectively. The circumferential magnetic field is static, while the axial one is dynamic. As shown in Fig. 2, a 70-mm-wide and 0.15-mm-thick iron-cobalt alloy patch, used to amplify the magnetostrictive effect, was bonded in the circumferential direction to the pipe with epoxy glue. A pair of magnets was placed on top of the patch to achieve a uniform and relatively strong circumferential static magnetic field therein. A 40-finger solenoid coil was wound over the patch to generate an axial dynamic magnetic field and then either excite waves in the patch or sense them by the receiving transducer. To excite a pure torsional guided wave in the pipe, the density of the current applied to the coil was chosen carefully to generate an axial magnetic field of comparable magnitude with that of the static circumferential magnetic field.

The experiments were performed on a straight pipe and two bent pipes with bending angles of 90° and 180°, respectively. The dimensions and material properties of the pipes were the same as those in Sec. 2.

3.2. Experimental results and analysis

A five-circle square pulse was used in the experiments. The exciting and receiving transducers were placed at the same end of the pipe, and the received signals were filtered by a band-pass filter to reduce noise. The excitation frequency was 20 kHz, 30 kHz, or 40 kHz. Figure 3 shows the testing signals used for the straight pipe. At each excitation frequency, a relatively pure T(0,1) mode was excited in the pipe, thereby making this type of magnetostrictive patch transducer suitable for the following experiments. Other than the T(0,1) mode, another small signal can also be observed, indicated by the cycles in Fig. 3. The mode of this signal can be determined by its flying times of approximately 2.2 ms, 2.3 ms, and 2.5 ms for one trip of 5500 mm, which correspond roughly to the group velocities of the F(1,1) mode at 20 kHz, 30 kHz, and 40 kHz, respectively. Thus, we concluded that the flexural F(1,1) mode is also excited in this experimental setting.

Figures 4 and 5 show the testing signals used for the pipe bends with bending angles of 90° and 180°, respectively. Compared to those in Fig. 3 for the straight pipe, the testing signals for the pipe bends are more complicated and difficult to interpret.

In general, the end reflections of the T(0,1) mode are observed clearly in the testing signals, and the of T(0,1) mode decays faster in bent pipes than it does in the straight pipe, especially for the 180° bent pipe. This indicates that mode conversions are taking place, and more energy has been transferred to the converted mode.

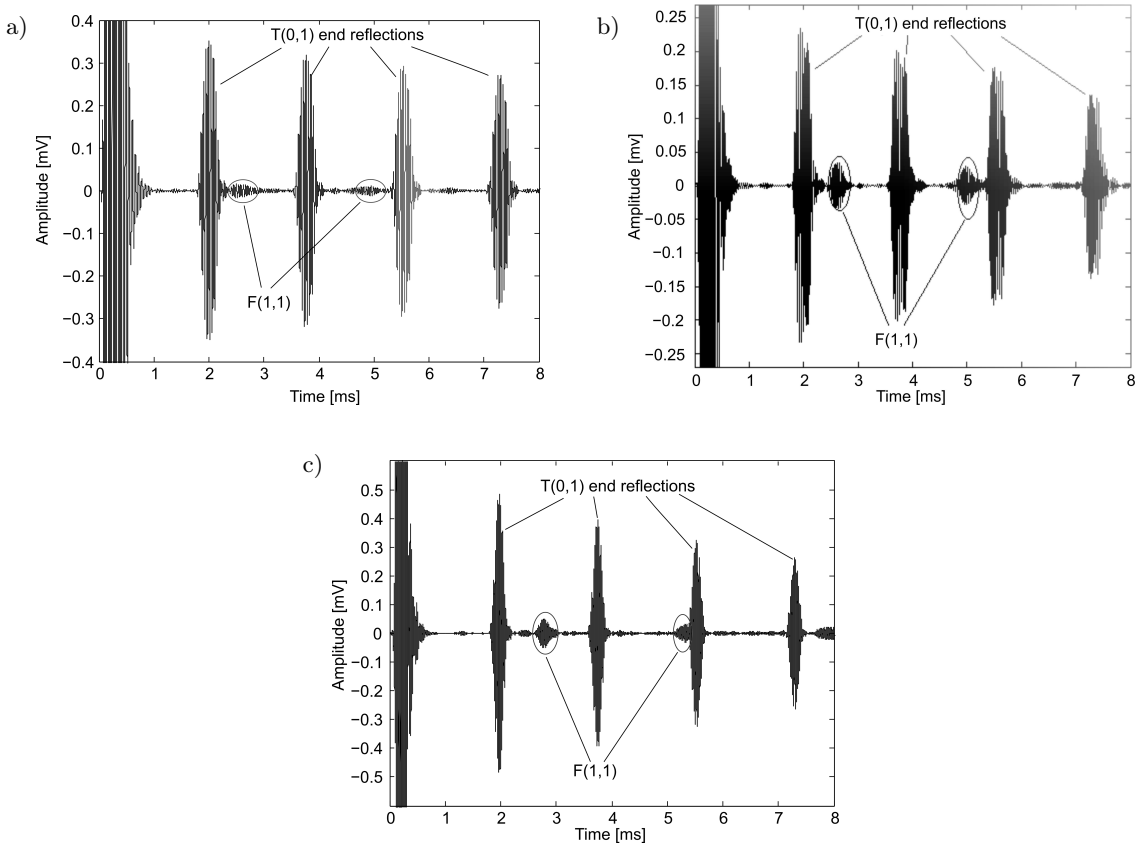

Fig. 3. Testing signals for the straight pipe at frequencies of: a) 20 kHz, b) 30 kHz, and c) 40 kHz.

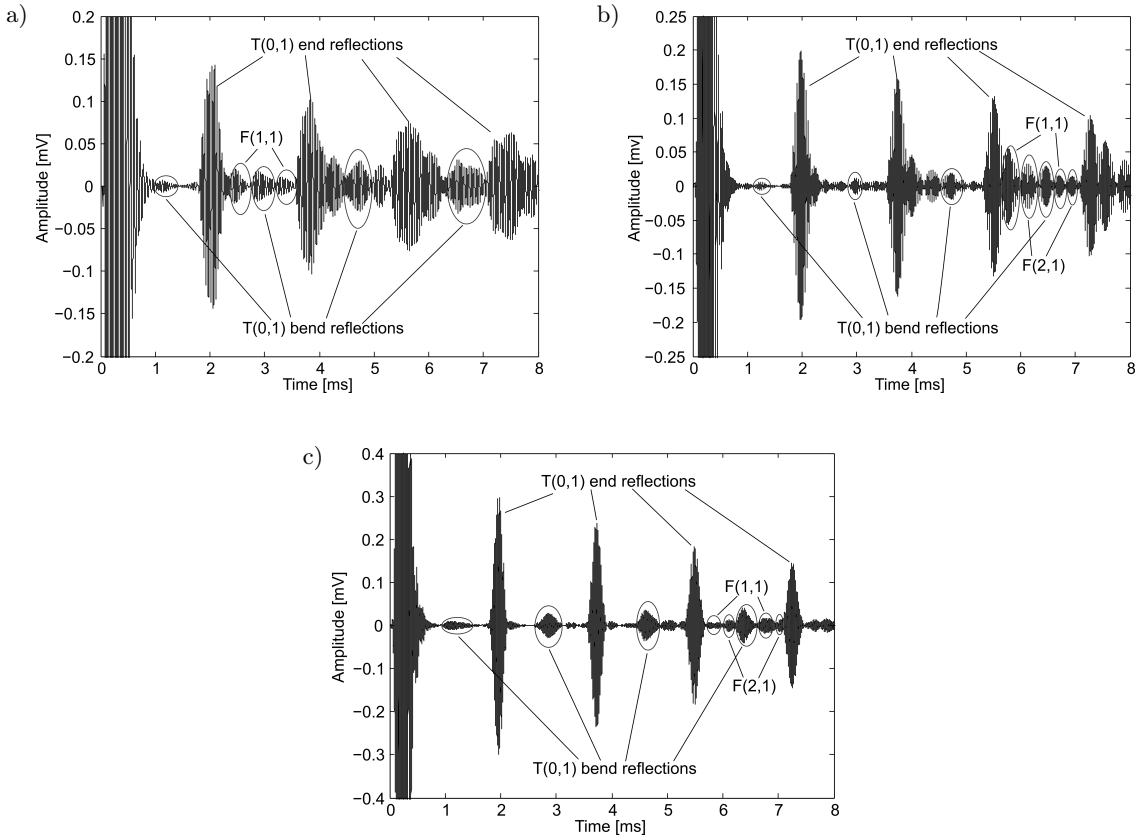

Fig. 4. Testing signals of the bent pipe with a bending angle of 90° at frequencies of: a) 20 kHz, b) 30 kHz, and c) 40 kHz.

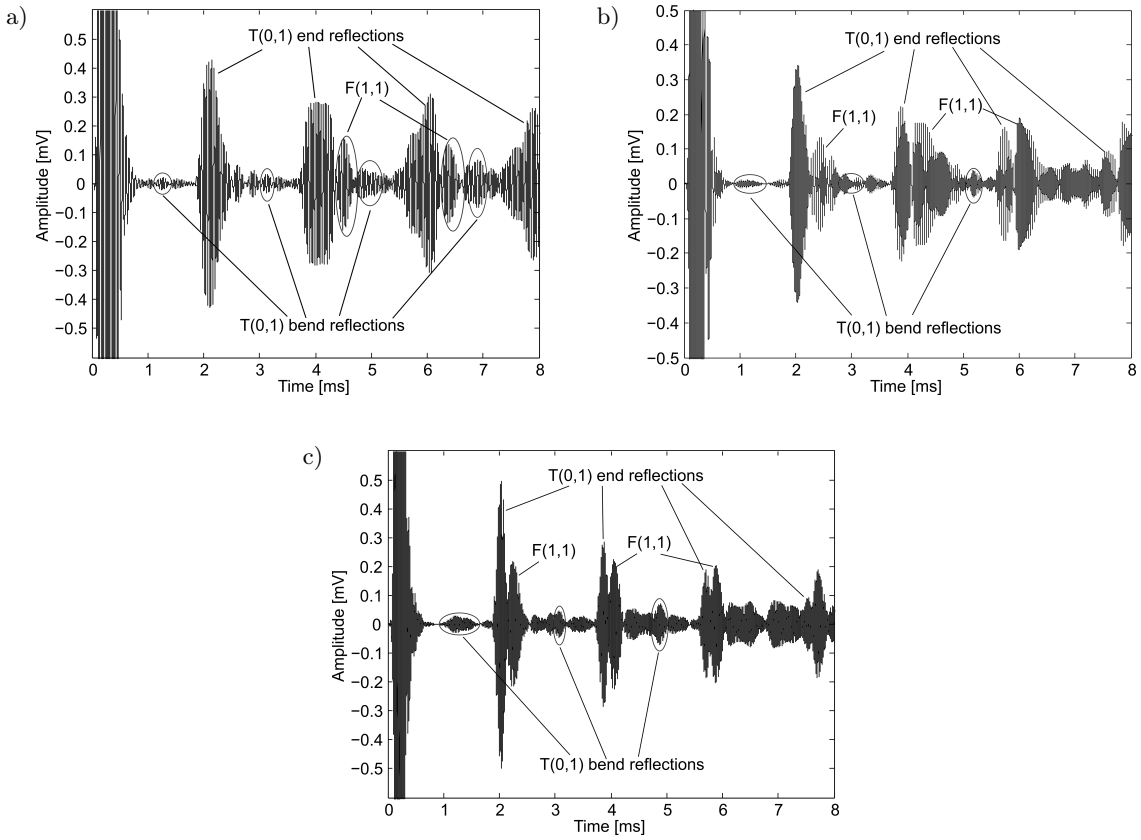

Fig. 5. Testing signals of the bent pipe with a bending angle of 180° at frequencies of: a) 20 kHz, b) 30 kHz, and c) 40 kHz.

In the case of the 90° bent pipe, as shown in Fig. 4, a weak signal is detected before the first end reflection of the T(0,1) mode, whereas no such signals are observed in Fig. 3, indicating the bend reflection of the T(0,1) mode. This is further confirmed by the signals that appear regularly in the middle of every two successive T(0,1) end reflections because the bend is in the middle of the pipe. The T(0,1) bend reflections increase with increasing propagation distance, which is because reflections occur every time the T(0,1) mode travels across the bend and overlaps each other. The amplitude of the T(0,1) bend reflections is also found to increase with increasing frequency, implying that more energy is reflected by the bend with increasing of excitation frequency of the T(0,1) mode.

As well as the T(0,1) reflections, other mode-converted signals can be seen in Fig. 4. According to the dispersion curves of the straight pipe (Fig. 1a), the frequency range of 20–40 kHz contains four modes, namely L(0,1), T(0,1), F(1,1), and F(2,1). Therefore, L(0,1), F(1,1), and F(2,1) are the potentially converted modes. The mode shape of L(0,1) differs completely from that of T(0,1), and thus the possibility of converting the T(0,1) mode into L(0,1) is slight. First, we focus on Fig. 4b because the signals seem to overlap less with each other, thereby facilitating analysis. As well as the T(0,1) bend-reflection signal located in the middle, four other signals can be observed between the two T(0,1) end reflections. The time differences between the end reflections and these four following signals are approximately 0.24, 0.56, 1.2, and 1.47 ms, respectively. According to Fig. 1a, the theoretical group velocities of T(0,1), F(1,1), and F(2,1) at 30 kHz are approximately 3200, 2390, and 1520 m/s, respectively. In one round of T(0,1) propagation, the incident T(0,1) travels across the bend twice, and hence mode conversions occur twice. For the first time of traveling through the bend, the possible converted modes of F(1,1) and F(2,1) travel three-quarters of the length of one 5500-mm round, whereupon the time differences between the T(0,1) end reflection and the converted modes of F(1,1) and F(2,1) are 1.34 and 1.42 ms, respectively. In the same way, the time differences between the T(0,1) end reflection and the converted modes of F(1,1) and F(2,1) for the second time are 0.15 and 0.47 ms, respectively. Then, considering the errors between the theoretical group velocities and the practical ones, as well as the dispersion and overlap of signals, which confuse the flying time of the signals, the theoretical time differences are agree well with those of the testing signals. Therefore, we conclude that these four signals are F(1,1), F(2,1), F(1,1), and F(2,1), as indicated in Fig. 4b.

All the mode-converted signals increase in amplitude with increasing propagation distance because energy is converted every time the T(0,1) mode passes through the bend. Another interesting phenomenon found in Fig. 4b is that the amplitudes of F(1,1) and F(2,1), mode-converted at the time when T(0,1) travels backward and through the bend, seem much larger than those of F(1,1) and F(2,1) modes, mode-converted when T(0,1) travels forward and through the bend. This may be due to the dispersions of these two flexural modes. These two flexural modes are dispersive according to Fig. 1a. Thus, the wave that propagates the shorter distance has a larger amplitude than the one that travels farther.

Mode-converted signals are also observed in Figs 4a and 4c. Because the F(2,1) mode is highly dispersive at 20 kHz, which is also close to the cut-off frequency of F(2,1), the mode conversion from T(0,1) to F(2,1) is weak and cannot be observed in Fig. 4a. Hence, we can observe three signals between two T(0,1) end reflections including the F(1,1), T(0,1) bend-reflection, and F(1,1) signals. The four converted signals are also found between the two T(0,1) end reflections in Fig. 4c, which coincide with those in Fig. 4b. However, the amplitudes of these mode-converted signals are much smaller than those of their corresponding signals in Fig. 4b. Therefore, we can conclude that the mode conversions are getting smaller with increasing excitation frequency.

As for the inspection of bent pipes with a bending angle of 180°, the testing signals, as shown in Fig. 5, are much more complicated than those for the bending angle of 90°. This is because the wave modes in pipe bends are much more dispersive according to the dispersion curves in Fig. 1b. Thus, the doubled length of the bent path leads to more dispersed signals and stronger overlaps, resulting in signals that are much more complicated.

The T(0,1) bend reflections can also be observed in Fig. 5, whose amplitude increases with the increase of propagation distance and excitation frequency. The mode-converted signals overlap strongly with each other and are therefore difficult to distinguish. Closely following the T(0,1) end reflections, all three parts of Fig. 5 contain an interesting mode-converted signal with a significant amplitude, which is found to be the F(1,1) mode by its flying time.

4. Conclusions

Because the axis of a pipe bend is curved, the wave behavior therein is considerably more complicated than that in a straight pipe, thereby motivating further study of the interaction between a pipe bend and the commonly used probing modes. The torsional T(0,1) mode is used most because of its non-dispersive nature. In this study, we focused on the wave behavior of the T(0,1) mode at low frequencies in small-bore pipes. The dispersion curves for straight and bent pipes were calculated to interpret the testing signals. Experiments were conducted on a magnetostrictive system. A fairly pure T(0,1) mode was excited in the pipes by using a magnetostrictive patch type transducer. The T(0,1) bend reflection and the mode conversions from T(0,1) to F(1,1) and F(2,1) were observed in the testing signals. The magnitude of the T(0,1) bend reflections increased with the increase of propagation distance and excitation frequency. The amplitude of the mode-converted signals also increased with the increase of propagation distance, but it decreased with the increase of excitation frequency. The bent path in a pipe bend with a bending angle of 180° is longer than that in one with a bending angle of 90°. Hence, the testing signals for the 180° pipe bend were are much more complicated than those for the 90° one because the wave modes in a pipe bend are highly dispersive. Therefore, scanning the pipe bends with larger bending angles is more difficult.

Acknowledgments

This work was supported by the National Natural Science Foundation of China (No. 51709216) and the Fundamental Research Funds for the Central Universities (WUT:2020III007XZ).

References

1. Bao X.L., Raju P.K., Uberall H. (1999), Circumferential waves on an immersed, fluid-filled elastic cylindrical shell, *Journal of the Acoustical Society of America*, **105**(5): 2704–2709, doi: 10.1121/1.426887.
2. Demma A., Cawley P., Lowe M.J.S., Pavlakovic B. (2005), The effect of bends on the propagation of guided waves in pipes, *Journal of Pressure Vessel Technology*, **127**(3): 328–335, doi: 10.1115/1.1990211.
3. Demma A., Cawley P., Lowe M.J.S. (2001), Mode conversion of longitudinal and torsional guided modes due to pipe bends, *AIP Conference Proceedings*, **557**(1): 172–179, doi: 10.1063/1.1373756.
4. Hayashi T., Kawashima K., Sun Z.Q., Rose J.L. (2005), Guided wave propagation mechanics across a pipe elbow, *Journal of Pressure Vessel Technology*, **127**(3): 322–327, doi: 10.1115/1.1990210.
5. He C., Wu B., Fan J. (2001), Advances in ultrasonic cylindrical guided waves techniques and their applications [in Chinese], *Advances in Mechanics*, **31**(2): 203–214.
6. Loveday P.W, Long C.S., Ramatlo D.A. (2018), Mode repulsion of ultrasonic guided waves in rails, *Ultrasonics*, **84**: 341–349, doi: 10.1016/j.ultras.2017.11.014.
7. Maze G., Léon F., Ripoche J., Überall H. (1999), Repulsion phenomena in the phase-velocity dispersion

curves of circumferential waves on elastic cylindrical shells, *Journal of the Acoustical Society of America*, **105**(3): 1695–1701, doi: 10.1121/1.426708.

8. Nishino H., Yoshida K., Cho H., Takemoto M. (2006), Propagation phenomena of wideband guided waves in a bended pipe, *Ultrasonics*, **44**: 1139–1143, doi: 10.1016/j.ultras.2006.05.155.
9. Rose J.L. (1999), *Ultrasonic waves in solid media*, Cambridge: Cambridge University Press.
10. Sanderson R.M., Hutchins D.A., Billson D.R., Mudge P.J. (2013), The investigation of guided wave propagation around a pipe bend using an analytical modeling approach, *Journal of the Acoustical Society of America*, **133**(3): 1404–1414, doi: 10.1121/1.4790349.
11. Ta D., Liu Z., He P. (2004), Optimal parameters of ultrasonic guided waves non-destructive testing in viscous liquid-filled elastic pipes [in Chinese], *Acta Acustica*, **29**(2):104–110.
12. Treyssède F. (2008), Elastic waves in helical waveguides, *Wave Motion*, **45**(4): 457–470, doi: 10.1016/j.wavemoti.2007.09.004.
13. Überall H., Hosten B., Deschamps M., Gerard A. (1994), Repulsion of phase-velocity dispersion curves and the nature of plate vibrations, *Journal of the Acoustical Society of America*, **96**(2): 908–917, doi: 10.1121/1.411434.
14. Verma B., Mishra T.K., Balasubramaniam K., Rajagopal P. (2014), Interaction of low-frequency axisymmetric ultrasonic guided waves with bends in pipes of arbitrary bend angle and general bend radius, *Ultrasonics*, **54**(3): 801–808, doi: 10.1016/j.ultras.2013.10.007.
15. Wu W., Wang Y. (2019), A simplified dispersion compensation algorithm for the interpretation of guided wave signals, *ASME, Journal of Pressure Vessel Technology*, **141**(2): 021204, doi: 10.1115/1.4042595.
16. Zhou W.J., Ichchou M.N. (2010), Wave propagation in mechanical waveguide with curved members using wave finite element solution, *Computer Methods in Applied Mechanics and Engineering*, **199**(33–36): 2099–2109, doi: 10.1016/j.cma.2010.03.006.